Ratings of Oil Power Transformer in Different Cooling Modes

Zoran Radakovic, Marko Sorgic, Wim Van der Veken, and Gert Claessens

***Abstract*—This case study shows the application of the calculation method based on the detailed thermal-hydraulic network model. The method is applied for the thermal design of oil power transformer of rated power 750 MVA in oil-directed, air-forced cooling mode; rated powers are also specified for oil-natural, air-forced and oil-natural, air-natural cooling modes. The results of the calculations using developed software for three cooling modes are compared with the results of the heat-run test of the transformer equipped with fiber-optic sensors. In addition to confirmation of the accuracy of the model, this paper demonstrates the full power of the integrated method (inner heating and outer cooling) for thermal calculations. All relevant components (pressure drops, oil flows, oil temperatures, etc.) in different cooling modes are obtained from the model and exposed in this paper.**

***Index Terms*—Hot-spot temperature, oil-directed, air-forced (ODAF) cooling, oil-natural, air-forced (ONAF) cooling, oil-natural, air-natural (ONAN) cooling, thermal design, transformer.**

I. Introduction

THE temperature in oil power transformers is the most important limiting factor for their loading. In the authors' previous papers [1], [2], the importance of having good methods and tools for thermal design of oil power transformers is explained. The conclusion is that these days, a detailed thermal-hydraulic network model (THNM) seems to be the optimal platform for tools for thermal design. The classical approach in the industry of power transformers, to use simplified expressions to calculate characteristic components (pressure drops and temperature differences) and to adjust coefficients in these expressions based on results of heat-run tests, has extreme limitations in accuracy and application to the cases not met in previous practice. The computational fluid dynamics (CFD) methods are identified as a good supporting tool for developing methods based on detailed THNM, but are not convenient to be applied for the thermal design of the complete transformer.

THNM does not deal with the calculation of temperatures in constructive parts of the transformer (i.e., with possible local overheating due to flux leakage and high losses in constructive parts), such as tank or clamping frame. This overheating is a matter of proper design and manufacturing of the core and shielding, not of the proper design of the cooling system.

The basic postulates of the theory can be found in [3]–[5]; in our previous papers [1], [2], the complete methodology was explained and some important details were discussed.

This paper represents the natural continuation of papers [1] and [2], and gives announced results of comparison with the values measured in the heat-run test. The details about the calculated and tested unit of high-power 750 MVA oil-directed, air-forced (ODAF) and with rated power of 600 MVA in oil-natural, air-forced (ONAF) and 450 MVA in oil-natural, air-natural (ONAN) cooling modes are given in Section II.

The details of the construction for which a certain approximation has been introduced are discussed in Section III. Section IV deals with the essential parameters of the model, which have a significant influence on the calculation results and which are a matter of quality control of the manufacturing of the conductor and the manufacturing of the transformer.

Section VIII contains the results and Section IX deals with the comparison of the results of the calculations for both heat-run tests (rated losses and rated current) in all three cooling modes (ODAF, ONAF, and ONAN) with measured data (top and bottom oil temperatures on the radiators, average winding temperature (via measured dc resistance using the UI method) and the temperatures at the top of the windings measured using fiber-optics sensors). Also, the results of the calculations of temperatures in real operation of the transformer loaded with rated current are given in Section VIII.

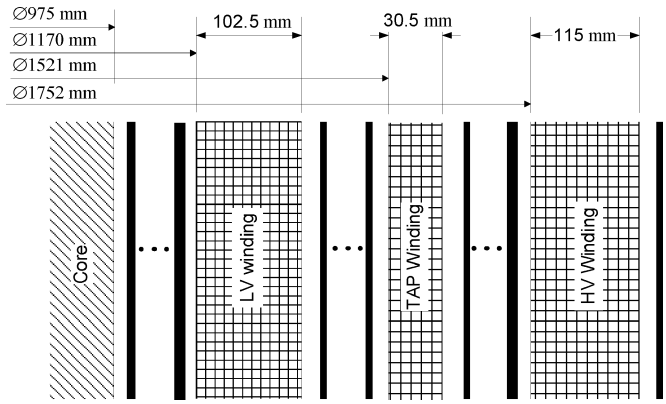

Fig. 1. Radial dimensions.

II. Data About the Transformer

The ratings of the transformer are: three-phase five-limb, 750-MVA, 230-kV/380-kV, YNa0d11, short-circuit voltage 10.5%. The radial dimensions are given in Fig. 1. The topology

Manuscript received January 11, 2011; revised May 24, 2011; accepted November 09, 2011. Date of publication December 29, 2011; date of current version March 28, 2012. Paper no. TPWRD-00025-2011.

Z. Radakovic and M. Sorgic are with the Faculty of Electrical Engineering, University of Belgrade, Belgrade 11000, Serbia (e-mail: radakovic@etf.rs; sorgic@etf.rs).

W. Van der Veken and G. Claessens are with CG Power Systems Belgium NV, Mechelen B-2800, Belgium (e-mail: wim.van.der.veken@cgglobal.com; gert.claessens@cgglobal.com).

Digital Object Identifier 10.1109/TPWRD.2011.2176543

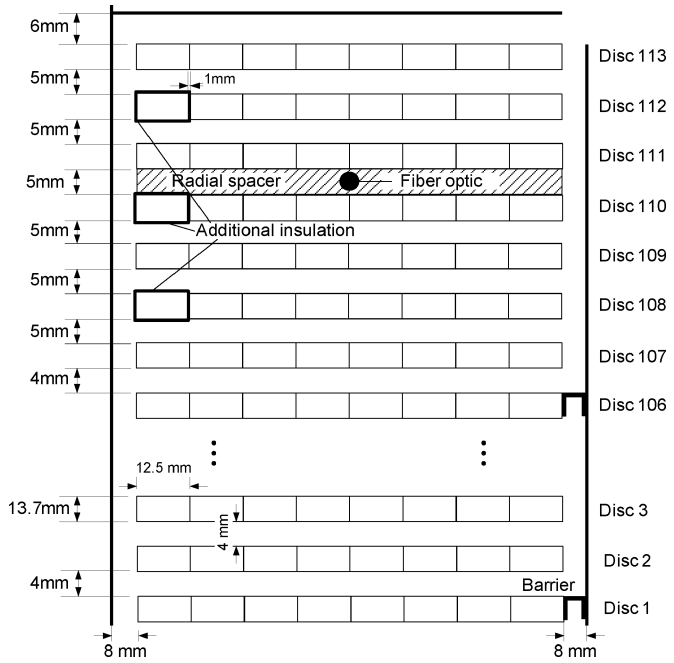

Fig. 2. Low-voltage (LV) winding.

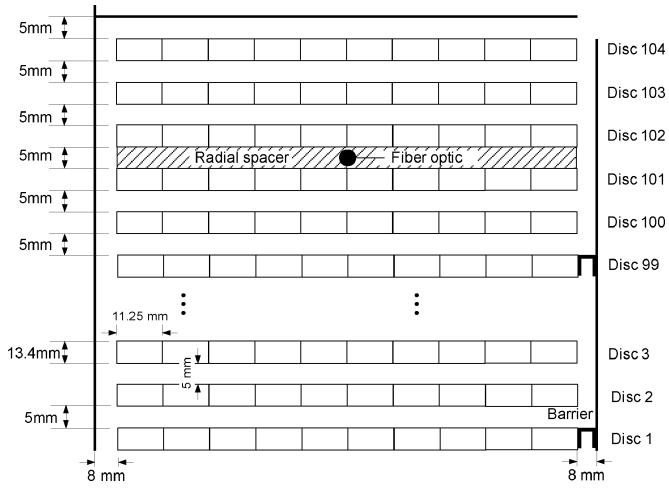

Fig. 3. High-voltage (HV) winding.

of the main windings—the low-voltage (LV) winding and high-voltage (HV) winding are given on Figs. 2 and 3, respectively. The tertiary winding (TV), being ON cooled, situated as the first winding to the core, is not included in the calculations since the losses in rated conditions are very low (3.11 kW per phase); the losses per phase in other windings are: 55 kW in LV, 33.7 kW in tap, and 154 kW in HV. The widths of the cooling ducts are given as design values (before pressing and without considering the bulging effect).

The insulation system below the LV winding is built in a way that practically no pressure drop on it exists. In other assemblies of insulation between the windings (LV, tap, and HV), the yoke pressure drop exists. These assemblies contain insulation rings and protection rings (potential rings) and are designed to ensure proper insulation levels according to manufacturer practice and rules.

The transformer contains no elements for adjusting oil distribution between the windings. Generally, this can be done by using the following element producing additional pressure drop: the aperture, the rings causing zig-zag oil flow, and the opening of controlled diameter and the length in support brackets (openings for injection of the oil from the oil distribution channel to the windings). All of these solutions can be applied for a group of windings and/or for each of the windings.

The transformer was filled with Nynas 3000 mineral oil.

The outer cooling is described in Section III-B.

III. Introduced Simplifications

All calculations are performed using the developed software, which treats numerous constructions used in practice. In this case study, there are details which are not exactly described in the software. This section specifies these details and the manner in how they are considered using the currently available options in the software.

A. Additional Insulation on Some of the Conductors

In LV and HV windings, additional insulation is used on some of the conductors. The form in the LV winding is shown in Fig. 2, while in the HV winding, protection caps (edge protection of width 10 mm) are used. This additional insulation is considered via thermal resistance to heat conduction (element of thermal network [1]) and in that way taken into account in thermal calculations, but is not included in the hydraulic network [1]; it is considered that the radial oil ducts are of constant width since in the software, there is no possibility of specifying the variable width of one radial cooling duct.

Edge protection in the HV winding is presented in the THNM as it covers a complete vertical surface of the conductor; it means that instead of covering 10 mm of the vertical surface and 10 mm of the horizontal surface, a complete vertical surface of 13.4 mm is covered while the horizontal surface has no additional thermal insulation.

B. Equivalent Uniform Radiator Battery

The software allows modeling of plate radiators, tubular radiators, fans blowing vertically, fans blowing horizontally, and fans blowing vertically and horizontally. Also, the software covers nine different topologies of positions of fans on the radiators, but it does not allow modeling of the case when there are differently cooled radiators. On the transformer, the radiators have either one or two fans. The radiators themselves are the same—there are 26 radiators with 28 plates. In addition to a nonequal number of fans, in heat-run tests, some of the fans on the radiators with one fan were turned off. For the real topology of the radiator bank being active during the heat-run test, the equivalent bank is taken, having the same number of AF and AN cooled plates; the number and type of fans (diameter 500 mm) is equal to the number and type of operating fans, the plate length, and the plate width, and the distance between the plates (45 mm) is the same as the real ones, but the number of plates per radiator is different from the real one. The equivalent radiator bank consists of 22 radiators, each one having 33 plates of width 520 mm and the length 3.4 m—13 plates are AF cooled (This is determined by the diameter of the fan.) and 20

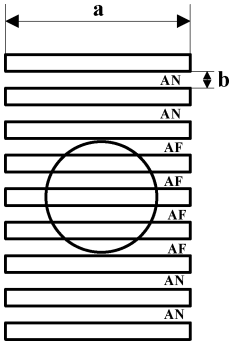

Fig. 4. Position of the fan blowing vertically with respect to the plates of the radiators.

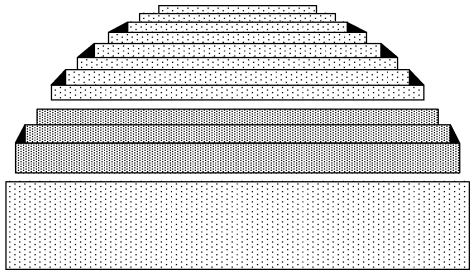

Fig. 5. Half of the core.

are AN cooled. From the point of view of cooling power, the approximation introduces no error, but the hydraulic resistance is slightly different from the real one.

The pressure drop on this part of the oil loop is calculated from the appropriate hydraulic network containing: the pipe for cold oil of diameter 260 mm and length 5.44 m, the pipe for hot oil of diameter 304 mm and the length 11.75 m), the pipes (collecting pipes) for cold and for hot oil holding the radiators (the distance between the pipes from the collecting pipe to the radiators is 580 mm, diameter 316 mm, total length 8 m), pipes from the collecting pipes to the radiators (diameter 80 mm, distance between the plates 45 mm), and the plates of the length 3.4 m. Local pressure drops on the pipes (curves, valves, etc.) are also included in the hydraulic network.

C. Air Flow Over the Radiator Plates

There is simplification in the software which is general and applied always when the cooling is with plate radiators and vertically blowing fans. For the calculation of the cooling power (it reflects to oil temperature and to pressures in oil in the radiators), air flow by AF-cooled plates is needed. (Based on air velocity, convection heat-transfer coefficients are determined.) The air flow is determined from the equilibrium of pressures produced by the fan and pressure drop in the vertical duct. Simplification is that uniform air flow is assumed over the cross section of the air duct $(a \times b)$; for the case presented in Fig. 4 if the air flow between the plates is Q_1, frictional pressure drop in the duct is calculated for air flow Q_1 (cross section $a \times b$, length 3.4 m). Pressure produced by the fan is calculated for air flow of $4 \cdot Q_1$.

D. Fixing of the Core

This is one more illustration about the level of details in applied detailed THNM. The function for calculating pressure drop and temperatures (of the surface and inside the core) assumes that the bandage is over the complete surface of the core. The hydraulic diameter is calculated for the cross section of oil consisting of oil ducts in the core (between the core sheets—in the example of the core with half of the core shown in Fig. 5 there are five ducts—the fifth is in the middle) and of small triangles formed between the bandage and the sheets. (It is assumed that there are not any wooden sticks.) The bandage is taken into account in thermal calculations—modeled by thermal resistance to conduction through the bandage added to thermal resistance to heat conduction along the sheet. For the last package of sheets (top package in Fig. 5), it is also added to the thermal resistance to heat conduction perpendicular to the sheet.

The core of the calculated transformer has somewhat different construction: some of triangles are filled by wooden sticks (see Fig. 5) and the bandage consists of four parts, covering just a part of the core. These details are not taken into account: the calculation is made for the configuration implemented in the function for the core. The software can be extended to cover the quoted real configuration, but this does not have significant influence. It is also important to understand that the model follows the detailed physics of heat transfer and can be easily extended to accurately describe some particular detail used by some specific manufacturer.

IV. Essential Parameters

This section discusses the most critical parameters in the application of the model. There are two major difficulties: 1) defining the bulging of the insulation and 2) evaluation of nonperfect sealing of the OD oil supplying system.

A. Bulging

This is a well-known phenomenon of reducing the cooling channels and effective increase of the thickness of the insulation and increase of the thermal resistance by CTC conductors. (CTC consists of many parallel-connected small conductors with a common outer insulation—for example: 39 enamel insulated conductors of the width 1.25 mm and the height 10 mm each, outer both side insulation thickness 1.5 mm, the outer conductor width 29.5 mm, and the height 21.7 mm.) Namely, by bending a conductor, the insulation changes the form (forms half-cylinder form) and partly closes the radial channel.

The quantification of the bulging is not so easy since it depends on the quality of the conductor. It is known from practice that there were serious problems with the conductor of some manufacturers: if the bulging is too big, the extreme reduction of the radial cooling channels appears, causing an end effect increase of conductor temperature. So the accurate estimation of the bulging empirical equation should be established, depending on the manufacturer of the conductor and the characteristics of the conductor and the winding. The main issue is to collect data, through measurements on real windings.

TABLE I
ESTIMATED BULGING BY CTC CONDUCTORS

	LV	Tap	HV
Insulation thickness (mm)	1	1.5	1.1
Width of the conductor (mm)	12.5	29.5	11.25
Bulging (mm)	0.59	0.8	0.60
Reduction of cooling channel (mm)	1.19	1.6	1.19

In transformer engineering, there is an approximate procedure of estimating the bulging: the increase of insulation thickness by CTC conductors depends on insulation thickness and the width of the conductor. The results of the application are given in Table I. Please note that LV and TAP windings are made of CTC conductor, while one-third of the HV winding (its middle part) is made of twin conductor—there is no bulging in the zone of twin conductors.

B. Nonperfect Sealing

This is also a practical issue—theoretically the OD transformer should be sealed well (i.e., there should be no leakage of oil out of the active parts.) (Complete upstream oil flow should be through the active parts.) If some oil flow for non-OD-cooled elements of the OD-cooled transformer (some of the windings and/or the core) is needed, openings in the oil distribution channel can be designed to achieve aimed oil flow through non-OD-cooled elements.

In the software, perfect sealing is assumed, but it is possible to specify the number and the diameter of the openings on the oil distribution channel. The appearance of these openings causes the appearance of oil bypass (i.e., nonperfect sealing can be modeled). Varying the number and the diameter of the opening, the oil bypass changes.

Real sealing is a practical problem and a quality issue and it is hardly possible to predict or model it accurately. The next inconvenience is that the flow of oil bypass cannot be checked directly (it cannot be measured). The check can be done indirectly; there are two options to do it in the phase of performing the short-circuit heat-run test, where the total oil flow through the cooler is also measured: 1) to measure the oil temperature at the top of each winding (using fiber optics) and to calculate the oil flow through each winding using this temperature and the values of the losses and 2) to calculate oil flows through each of the windings using detail THNM. Option 1) is more reliable, since there is only simple single calculation step to get the flows from the measured temperatures. For both options, the flow of oil bypass is determined as the difference between the flow through the cooler and the sum of flows through the windings.

Since in the transformer the fiber-optic sensors are built only in the winding (to measure the conductor temperature), it was only possible to use option 2) to estimate the oil bypass flow.

It was performed in the following way: the number and diameters of the openings on the oil distribution channel were changing until the total oil flow from the cooler became equal to the measured value. The flow of oil bypass is obtained by subtracting the calculated oil flows through the windings from the flow through the cooler.

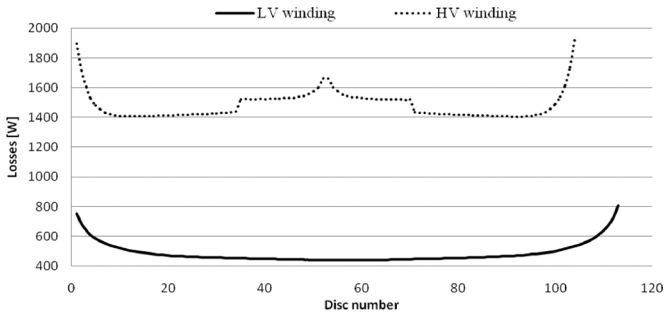

Fig. 6. Distribution of the power losses over discs.

TABLE II
INPUT VALUES OF POWER LOSSES

	ODAF	ONAF	ONAN
Rated winding losses (kW)	729.1	466.6	262.5
Stray flux losses (kW)	125.5	79.9	44.9
Sun irradiation (kW)	78	0	0

V. POSITION OF FIBER-OPTIC SENSORS

The position of six built in fiber-optics sensors is as follows: two in each phase, one of them in the LV winding (see Fig. 2) and one in the HV winding (see Fig. 3). The sensors are positioned in the middle of the spacer between the third and the fourth discs from the top. The thermal calculations described in this paper were done after the transformer was produced. That is why the sensors are not positioned at the locations where the hot spot is expected according to the calculations: for the LV winding at the top disc and for the HV winding in the second conductor above the barrier for the zig-zag oil flow positioned in the middle area of the winding. (This position slightly varies with the cooling mode.)

VI. POWER LOSSES

The power losses used for the calculation of temperatures at the ODAF cooling mode are as follows: in the windings—total losses at rated current 729.1 kW (distribution of the losses is shown in Fig. 6), the no-load losses 145.2 kW, the losses due to stray flux 125.5 kW, and the absorbed heat of sun irradiation 78 kW. The losses due to stray flux are obtained as the difference of the measured losses in the short-circuit test and the calculated losses in the winding.

The losses in the conductors are obtained from the software for the calculation of power losses. Since in the moment of the calculation of the losses the temperature distribution is not known, the losses are calculated at a uniform temperature of all conductors, being equal to the rated winding temperature. The next accuracy level of the calculation can be achieved by recalculating previously mentioned values to the temperature of each conductor, obtained using detailed THNM. For practical reasons, this recalculation, as the shell calculation loop, has to be based on a simple equation. (There is a linear increase of dc losses and a decrease of additional losses with the temperature.) This shell loop is implemented in the calculation method, but

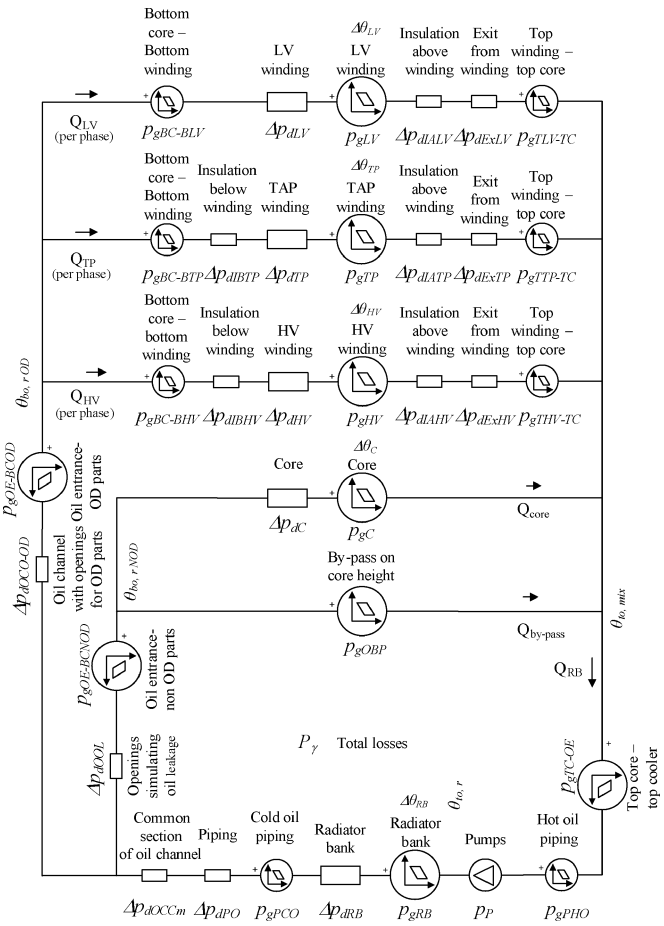

Fig. 7. Hydraulic network of the transformer in normal operation. ϑ—oil temperature (^{0}C), $\Delta\theta$—oil temperature gradient (in Kelvin), p_g—component of gravitational pressure, Δp_d—component of pressure drop (frictional and local), Q—oil flow (m^3/h), Key: RB—cooler (in this case, the radiators), HV—high-voltage windings, TP—tap windings, LV—low-voltage windings, OBP—oil bypass on a height from the bottom to the top of the core, C—core from the bottom to the top, TC-OE—from the top of the core to the exit of oil from the tank, PHO—pipes for hot oil, P—pump, PCO—pipes for cold oil, PO—complete pipes for oil, OCCm–common section of oil channel, OE-BCOD—from the entry of the oil to the tank to the bottom of the core for OD-cooled parts, OE-BCNOD—from the entry of the oil to the tank to the bottom of the core for non-OD-cooled parts, OOL—openings of oil leakage, OCO-OD—oil channel with openings for OD cooled parts, EC—entry to the core, EnW—entry to the winding, BC-BW—from bottom of the core to the bottom winding, IBW—insulation below the winding, W—winding (LV, TP or HV), IAW—insulation above the winding, ExW—exit from the winding (under pressing ring), TW-TC—from the top of the winding to the top of the core, bo, r_{NOD}—bottom oil entering non-OD-cooled parts, bo, r_{OD}—bottom oil entering OD-cooled parts, to mix—mixture of oil exiting the active part and oil bypass, to the r—top oil at the entrance to the radiator.

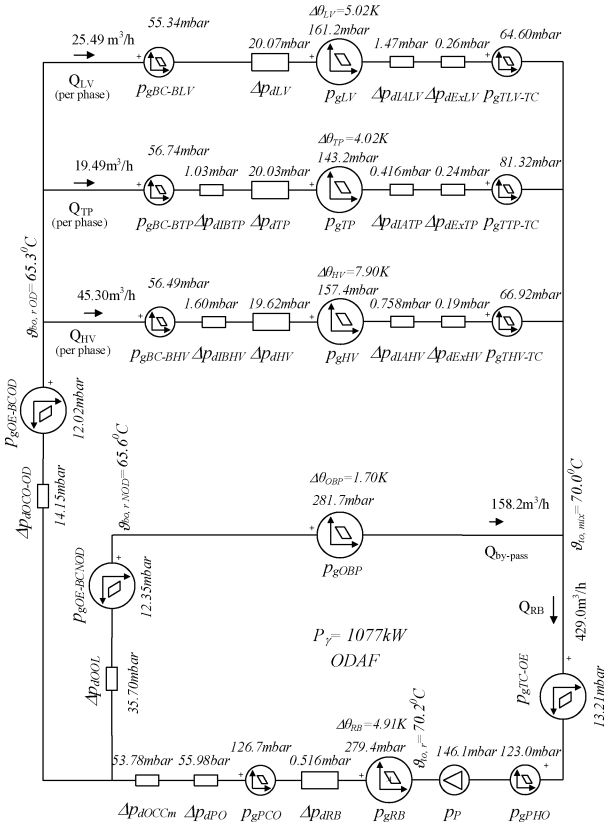

Fig. 8. Characteristic quantities for oil (ODAF, total rated losses).

is not activated, since it prolongs the computing time. It is estimated that there is no sense to perform these iterations before there is evidence of high accuracy of the value of losses in each conductor delivered by the software for the calculation of power losses. In this case, the RI^2 losses and supplementary losses are calculated with the Magnaxi software [6]. This is 2-D electromagnetical finite-element method software, which is developed within the CG Company. This software has been benchmarked with other well-known software, such as the Anderson, Rabins and Roth software and the measurement data of a large number of transformers.

Since the detailed THNM uses the data in parts of the core and in each of six surfaces of the tank [2], the distribution of the stray flux losses and absorbed sun irradiation is specified as input data. Without calculating the distribution of stray flux losses using some finite-element method, it is not possible to allocate them—the losses in the tank or constructive parts inside the tank. This allocation is important since it also influences the oil distribution, first of all, via oil temperatures and gravitational pressure components: for example, putting all stray flux losses into the tank walls increases oil bypass. The results for ON cooling exposed in the paper are obtained under conditions that stray flux losses are distributed equally under the LV, tap, and HV windings (for example, the ONAF cooling mode and heat-run test with total losses: under each winding 79.9 kW/9= 8.88 kW). Table II presents the input data for the losses and additional heating due to the sun irradiation. The solar radiation on the transformer cover and irradiated walls (tank size is 10.1 $\times$ 3 $\times$ 3.65 m) and the radiators bank is taken to be equal to 78 kW. These extra losses are only added during testing in the highest cooling stage per agreement with the customer. So in the first part of the heat-run test (total rated loses) in the ODAF cooling mode, the losses are equal to the sum of rated winding losses, rated stray losses, rated core losses, and adopted sun irradiation.

For the calculation of the transformer in real rated operation, no-load losses are distributed along the parts of the core.

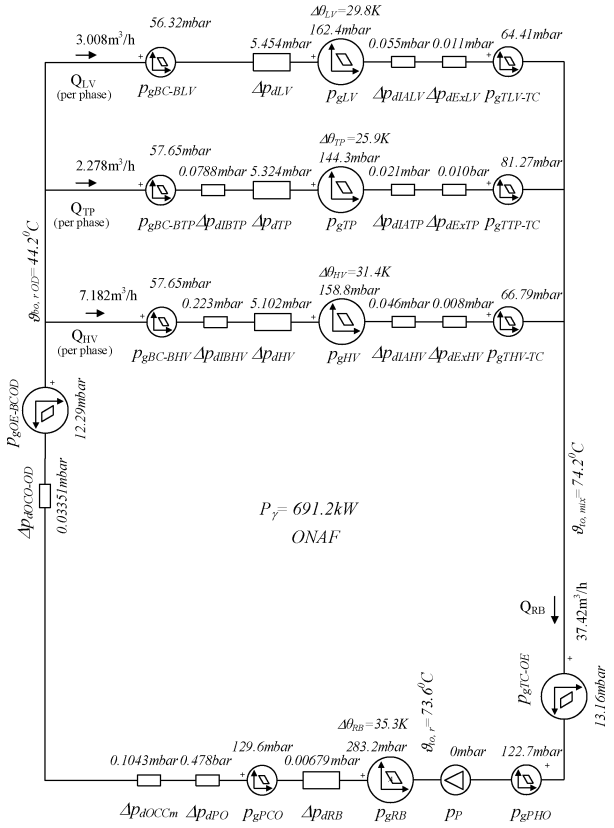

Fig. 9. Characteristic quantities for oil (ONAF, total rated losses).

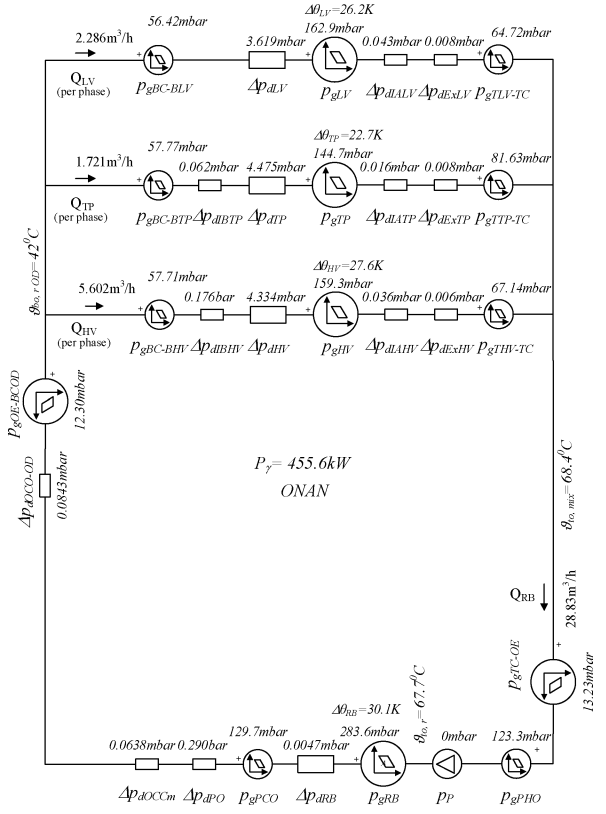

Fig. 10. Characteristic quantities for oil (ONAN, total rated losses).

VII. Hydraulic Network of the Transformer

The hydraulic network of the transformer is shown in Fig. 7. It is similar to the network presented in [2], with the difference that in this case, the core is not OD cooled.

The hydraulic network from Fig. 7 corresponds to the ODAF cooling mode and normally loaded transformer. In the ONAF and ONAN modes, there is no pressure produced by the pump. (It is equalized with zero.) For the case of heating the transformer in the short-circuit heat-run test conditions, the branch of the core (parallel to the branch of the oil bypass) is omitted; the flow through the non-OD-cooled core is equal to zero in short-circuit heat-run test conditions [i.e., it starts when the losses in the core appear (real operating conditions)].

VIII. Results

Figs. 8–10 present the pressure drops, the oil flows, and some of the temperatures of oil, obtained by the calculation for rated losses in all three cooling modes, injected in the winding in the short-circuit heat-run test. In order to illustrate the component of oil flow through the core (see Section VII), Fig. 11 presents the same form of the calculation results for the rated load of the grid-connected transformer.

Tables III–V show the results of temperature calculations: 1) in heat-run tests at rated losses—column $P_{\gamma r}$; 2) in the heat-run test at rated current—column I_r; 3) for simulated normal operating conditions—according to the procedure from standards [7]—column "Simulated rated load [7]"; and 4) in real operation with rated load and losses existing in the windings and in the core—column "Normal rated load." In addition to the results of the calculations, the table presents the measured temperatures and the gradients obtained from the measurements $(^*)$ in the heat-run test with rated losses—the second number in the cells.

The results exposed in this section show characteristic values in different cooling modes ODAF, ONAF, and ONAN of the construction with oil guiding directly to the winding (OD construction). The basics of the methodology are explained in [1] and [2]: pressure equilibrium and its simplified (easy to understand) presentation in [1] and the details about OF construction, with running pumps (OF mode) and without running pump (ON mode) are considered in [2]. As expected, each component of oil flow drops drastically when the pump is switched off.

It is interesting to note that there is a difference between the temperatures obtained for normal operating conditions using the method from standard [7] and obtained by the calculation of the normally operating transformer. This difference increases with the decrease of the ratio of winding to core losses. (The biggest difference is for ONAN cooling). This is a consequence of changed distribution of oil flow in the transformer: the new component of oil flow appears in normal loading conditions: oil flow through the core; the oil heats up due to the losses in the core and this causes the reduction of the gravitational component of pressure and the appearance of oil flow through the core. This result points out that the procedure from [7] should be analyzed—this is the issue of further research, where using detailed THNM can be advantageous.

When performing the calculations, it was observed that the distribution of stray losses (especially in ONAN cooling mode) influences the calculation results; introducing the losses in tank

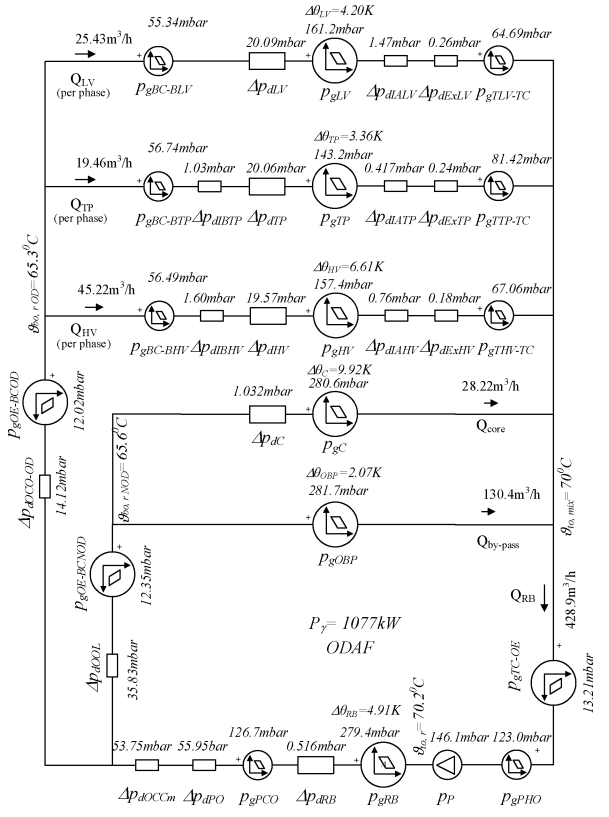

Fig. 11. Characteristic quantities for oil (ODAF, normal rated operation).

TABLE III
RESULTS OF THE ODAF COOLING MODE (750 MVA)

		P_{yr}	I_r	Simulated rated load [7]	Normal rated load
Oil flow	m^3/h	429	427		428.9
Losses	kW	1078	933	1078	1078
ϑ_{ao}	^{0}C	67.8/66.9*	63.2	67.8	67.8
ϑ_{to}	^{0}C	70.2/69.5*	65.4	70.2	70.2
$\vartheta_{Cu\,a,\,HV}$	^{0}C	82.3/92.2*	74.6	79.2	78.9
$\vartheta_{Cu\,a,\,LV}$	^{0}C	76.9/83.6*	70.4	75	74.4
$(\vartheta_{Cu\,a}-\vartheta_{ao})_{HV}$	K	14.5/25.3*	11.4	11.4	11.1
$(\vartheta_{Cu\,a}-\vartheta_{ao})_{LV}$	K	9.1/16.7*	7.2	7.2	6.6
$\vartheta_{Cu\,hs,\,HV}$	^{0}C	104	91.3	96.2	97.2
$\vartheta_{Cu\,hs,\,LV}$	^{0}C	92.8	84.3	89.1	88.3
H_{HV}		2.32	2.28	2.28	2.42
H_{LV}		2.48	2.62	2.62	2.7
$\vartheta_{Cu\,Fiber\,HV}$	^{0}C	96/103.6*	86.5		90.8
$\vartheta_{Cu\,Fiber\,LV}$	^{0}C	90.3/93.9*	82		86.1

H – hot-spot factor, calculated as $(\vartheta_{Cu\,hs}-\vartheta_{to})/(\vartheta_{Cu\,a}-\vartheta_{ao})$
Indexing key:
Cu a – average winding temperature
Cu hs – hot-spot winding temperature
Cu Fiber – local temperature at fiber position
* – Values obtained from the measurements

vertical walls causes the appearance of oil bypass. The consequences are higher oil flow through the radiators. That is why the distribution of stray flux and consequent losses should be defined as accurate as possible. The model we developed relates to hydraulic and thermal calculations based on the detailed description of physics; naturally, it has to be followed by accurate and detailed calculation of the losses.

TABLE IV
RESULTS OF THE ONAF COOLING MODE (600 MVA)

		P_{yr}	I_r	Simulated rated load [7]	Normal rated load
Oil flow	m^3/h	37.42	33.07		48.34
Losses	kW	691.2	546.5	691.2	691.7
ϑ_{ao}	^{0}C	55.9/54.9*	51.1	55.9	55.5
ϑ_{to}	^{0}C	73.6/68.2*	67.1	73.6	69.2
$\vartheta_{Cu\,a,\,HV}$	^{0}C	67/66.2*	59.8	64.6	67.7
$\vartheta_{Cu\,a,\,LV}$	^{0}C	65.4/63.8*	59.1	63.9	67.1
$(\vartheta_{Cu\,a}-\vartheta_{ao})_{HV}$	K	11.1/11.3*	8.7	8.7	12.2
$(\vartheta_{Cu\,a}-\vartheta_{ao})_{LV}$	K	9.5/8.9*	8	8	11.6
$\vartheta_{Cu\,hs,\,HV}$	^{0}C	94.6	83.7	93.5	93.3
$\vartheta_{Cu\,hs,\,LV}$	^{0}C	91.5	81.1	98	89.8
H_{HV}		2.13	2.29	2.29	2.59
H_{LV}		2.74	3.05	3.05	2.7
$\vartheta_{Cu\,Fiber\,HV}$	^{0}C	91/84.5*	80.5		90
$\vartheta_{Cu\,Fiber\,LV}$	^{0}C	88/79.9*	78.2		87.8

TABLE V
RESULTS OF THE ONAN COOLING MODE (450 MVA)

		P_{yr}	I_r	Simulated rated load [7]	Normal rated load
Oil flow	m^3/h	28.88	23.37		40.53
Losses	kW	455.6	307.4		452.6
ϑ_{ao}	^{0}C	52.7/54*	45.1	52.7	56.9
ϑ_{to}	^{0}C	67.7/64.8*	57.8	67.7	67.6
$\vartheta_{Cu\,a,\,HV}$	^{0}C	59.8/61.1*	49.9	57.5	63.8
$\vartheta_{Cu\,a,\,LV}$	^{0}C	58.8/59.6*	49.9	57.5	63.9
$(\vartheta_{Cu\,a}-\vartheta_{ao})_{HV}$	K	7.1/7.1*	4.8	4.8	6.9
$(\vartheta_{Cu\,a}-\vartheta_{ao})_{LV}$	K	6.1/5.6*	4.8	4.8	7
$\vartheta_{Cu\,hs,\,HV}$	^{0}C	82.7	67.9	81.5	83
$\vartheta_{Cu\,hs,\,LV}$	^{0}C	80.3	66.1	86.7	81.1
H_{HV}		2.41	2.88	2.88	2.74
H_{LV}		3.28	3.96	3.96	3.31
$\vartheta_{Cu\,Fiber\,HV}$	^{0}C	79.8/80.4*	66.1		81
$\vartheta_{Cu\,Fiber\,LV}$	^{0}C	77.6/78.1*	64.4		79.6

IX. CHECKING OF THE CALCULATION RESULTS

Tables III–V show not only the calculated values, but also the measured temperatures and the temperature gradients obtained from the measured temperatures.

Each table relates to one of three tested cooling modes: ODAF, ONAF, and ONAN; the measured temperatures are given for the total rated losses condition.

The following factors are possible sources of deviations of calculated from measured values: 1) number and diameter of holes used to model nonperfect sealing of the oil channel supplying the oil to the windings, 2) bulging of the insulation, and 3) equations for the convection heat-transfer coefficients. It appeared that the equation from [8] yields better results for OD cooling modes and from [4] for ON cooling modes, 4) inaccurate distribution of stray flux losses—this affects all temperatures especially in the ONAN cooling mode (see the end of Section VIII), and 5) possible omission in the measurements, for example, in selecting the points where top oil is measured or possible inaccuracy in determining the average winding temperature.

X. Conclusion

This is the first publication with the comparison of the calculated temperature using the design tool based on the detailed thermal-hydraulic network model of the oil power transformer. The case transformer is a big ODAF unit of 750 MVA, with rated powers of 600 MVA in the ONAF cooling mode and 450 MVA in the ONAN cooling mode. This unit is a representative and illustrative test example due to its high rating and variety of cooling conditions.

This paper shows the main advantages of the method for the thermal design of oil power transformers based on detailed THNM: it is integrated (The oil loop integrates inner heating and outer cooling parts.) and it is general. (It covers all kinds of cooling modes.) The integral and general character represent a significant advantage of such a method compared to the typical practice of using many small tools in the thermal design of a transformer: it simplifies the design process, saves time, and reduces the possibility of making mistakes. This paper shows that the method is fully based on physics and can take details in transformer construction into account. The method gives distribution of relevant quantities: flows and pressure drops in parts of a transformer and detailed distribution of oil velocities and temperatures inside the parts. This offers detection of the critical points and improvement and optimization of the cooling.

Possible sources of inaccuracy are quoted at the end of Section IX. These points are the subject of further development with the aim of increasing the accuracy and the reliability of the calculation method and the software for thermal design. Some details require an empirical approach (for example, defining bulging) and some of details analysis using finite-element software. Also, detailed THNM requires high quality and detailed data about the power losses. The next planned detailed checking of the model is on a big unit with fiber-optic sensors built also in the windings to obtain important value of the oil temperatures at the top of the windings.

The exposed results are the first ones when originally developed coefficients (based on experiments and CFD calculations) for local pressure drops in zig-zag cooled windings (corner and oil splitting/joining) are applied—this was one of the most important details studied after [2].

References

[1] Z. Radakovic and M. Sorgic, "Basics of detailed thermal-hydraulic model for thermal design of oil power transformers," *IEEE Trans. Power Del.*, vol. 25, no. 2, pp. 790–802, Apr. 2010.

[2] M. Sorgic and Z. Radakovic, "Oil forced versus oil directed cooling of power transformers," *IEEE Trans. Power Del.*, vol. 25, no. 4, pp. 2590–2598, Oct. 2010.

[3] K. Karsai, D. Kerényi, and L. Kiss, *Large Power Transformers*. New York: Elsevier, 1987.

[4] A. J. Oliver, "Estimation of transformer winding temperatures and coolant flows using a general network method," *Proc. Inst. Elect. Eng., C*, vol. 127, pp. 395–405, 1980.

[5] M. Yamaguchi, T. Kumasaka, Y. Inui, and S. Ono, "The flow rate in a self-cooled transformer," *IEEE Trans. Power App. Syst.*, vol. PAS-100, no. 3, pp. 956–963, Mar. 1981.

[6] R. Mertens, "Magnaxi," 2D e-m FEM Software (internal company document), Mechelen, 2001.

[7] *Power Transformers—Temperature Rise*, IEC Standard 60076-2, 1993.

[8] F. P. Incropera and D. P. DeWitt, *Heat and Mass Transfer*, 5th ed. Hoboken, NJ: Wiley, 2002.

Zoran Radakovic was born in Belgrade, Serbia, on May 27, 1965. He received the B.Sc., M.Sc., and Ph.D. degrees in electrical engineering from the University of Belgrade, Belgrade, in 1989, 1992, and 1997, respectively.

He was was a Research and Teaching Assistant at the University of Belgrade, as Humboldt Research Fellow at the University of Stuttgart, Stuttgart, Germany, and as Research and Development Engineer with Siemens AG, Nuremberg, Germany, responsible for the development of cooling in the technology and innovation department of the transformer division. Currently he is a Professor with the Faculty of Electrical Engineering, University of Belgrade.

Marko Sorgic was born in Pula, Croatia, on November 7, 1980.

He is a Research and Teaching Assistant at the Faculty of Electrical Engineering, University of Belgrade, Belgrade, Serbia. He has been working on his final thesis for about one year as a student trainee with Siemens AG, Nuremberg, Germany.

Wim Van der Veken was born in Diest, Belgium, on January 30, 1974. He received the B.Sc. and M.Sc. degrees in mechanical engineering from the University of Leuven, Leuven, Belgium, in 1994 and 1997, respectively.

After one year working as a Research Assistant at the University of Leuven, he joined CG Power Systems, Mechelen, Belgium, in 1998, where he began in the research-and-development team specializing in thermal and mechanical design. Later, he became Head of the mechanical engineering department and recently joined the product development team.

Gert Claessens was born in Willebroek, Belgium, on August 4, 1963. He received the M.Sc. degree in electrical/mechanical engineering from the Academy KIH De Nayer, Sint-Katelijne Waver, in 1986.

He joined CG Power Systems, Mechelen, Belgium, in 1989 as Design Engineer. Since 2006, he has been Head of the Electrical Engineering Department of Power Transformers.